

# High-Quality Protein Force Fields with Noisy Quantum Processors

Anurag Mishra\* and Alireza Shabani  
Qulab Inc., Los Angeles, California 90024, USA  
(Dated: 2019-10-31)

A central problem in biophysics and computational drug design is accurate modeling of biomolecules. The current molecular dynamics simulation methods can answer how a molecule inhibits a cancerous cell signaling pathway, or the role of protein misfolding in neurodegenerative diseases. However, the accuracy of current force fields (interaction potential) limits the reliability of computer simulations. Fundamentally a quantum chemistry problem, here we discuss optimizing force fields using scalable *ab initio* quantum chemistry calculations on quantum computers and estimate the quantum resources required for this task. For a list of dipeptides for local parameterizations, we estimate the required number of qubits to be 1576 to 3808 with cc-pVTZ(-f) orbital basis and 88 to 276 with active space reduction. Using a linear depth ansatz with active-space reduction, we estimate a quantum circuit with a circuit depth of few thousands can be used to simulate these dipeptides. The estimated number of 100s of qubits and a few thousand long circuit depth puts the pharmaceutical application of near-term quantum processors in a realistic perspective.

Structure and dynamics of proteins and other biomolecules determine their functioning role in living organisms. How a protein folds shapes its structure and its mechanistic interaction with other molecules in a cell. Therefore targeting biomolecules with abnormal behavior is a prime therapeutic approach. Since the early success of protein dynamics simulation [1, 2], computer simulation of biomolecules has been a cornerstone of structural biology and drug design [3]. The true dynamics of a protein system can be completely described by solving the time dependent Schrödinger equation to obtain the motion of nuclei and electrons. This is a quantum problem that requires *ab initio* quantum chemistry methods. While great advances have been made in the field, solving systems beyond  $\sim 50$  atoms remains an unfeasible task [4]. For dynamical systems, *ab initio* techniques remain unfeasible even at a small size.

In order to make useful computational predictions at a large size, one can further approximate the molecular system and assume that it is completely driven by Newtonian mechanics. Molecular dynamics (MD) applies classical mechanics to describe the dynamics and interactions of molecules [5]. Recent advances in free energy calculation has turned MD simulation into a reliable tool for *in-silico* drug discovery [6, 7]. MD finds wide applicability in various fields, and has been used for calculating protein folding kinetics [8], for computing ligand-protein binding energy [9], or deciphering CRISPR mechanism [10]. The multi-scale nature of these interactions, both in time and space, along with the complexity of biomolecules, demands a full-atomistic MD simulations. Over the years the accuracy of simulations have been significantly improved. However, toward a full predictive power, the accuracy and speed of computer simulation need further progress [11].

The accuracy of protein simulations relies on proper modeling of molecular interactions. An MD trajectory captures motion of atoms nuclei where the dynamics is governed by the energy potential shaped by the electronic

cloud. A common approach utilizes a classical potential function parametrized by local quantum chemistry calculations or experimental fitting, basically a hybrid quantum-classical approach [2, 12]. More recent theories suggest quantum perturbative methods (*ab initio* force-fields) [13] or neural networks to replace the classical potential function [14, 15].

Here, we focus on the MD simulations driven by classical potentials and force-fields and discuss how their quality can be improved by running *ab initio* quantum chemistry calculations on quantum computers. As an illustrative task, we focus our attention towards optimizing protein force field parameters via *ab initio* computations on a quantum computer. This task, while not impossible, is prohibitively expensive to tackle with classical computational techniques. Unlike a classical computer, the quantum resources to perform an *ab initio* computation scales linearly in the size of the problem [16, 17]. In this work, we first briefly review force field models for approximate calculation of the dynamics of a molecular system. We then discuss how *ab initio* quantum chemistry simulations can be used to improve protein force-field parameterization for more accurate MD simulations. We provide an estimate for the quantum resources required for to perform this task on near term quantum computers, and conclude with a discussion of other potential application of quantum computing to the field of biophysics. Additional details are provided in the Appendix. Our work shows that it is feasible to implement this illustrative task on the noisy intermediate-scale quantum (NISQ) computing era.

## Theory

**Force Field.** The potential energy surface (PES) of an atomic system describes its energy as a function of the chosen coordinates. A force-field (FF) tries to approximate the PES via a limited number of classical terms. The accurate PES depends on quantum mechanical ef-

fects, such as exchange repulsion, which have no classical analog. Thus, a complete and accurate description of the PES of a molecule with only a finite number of classical coordinates is an impossible task. Nevertheless, one can find a good approximation of this energy surface near the equilibrium where the configuration of the system is not too far from the stable configuration(s). A good FF model tries to balance multiple goals: it should use as little computational resources as possible to calculate the forces, it should describe the PES as accurately as possible and it should generalize over any possible combinations of atoms and configurations. As one can imagine, these goals are quite frequently in conflict with each other.

Common classical FF models are described by the potential [5, 18]

$$\begin{aligned}
 V = & \frac{1}{2} \sum_{i>j} k_{ij} (r_{ij} - \bar{r}_{ij})^2 + \frac{1}{2} \sum_i \tau_i (\theta_i - \bar{\theta}_i)^2 \\
 & + \frac{1}{2} \sum_{ni} V_{ni} (1 + \cos(n\omega_i - \bar{\omega}_i)) \\
 & + \sum_{i>j} \frac{q_i q_j}{r_{ij}} + \sum_{i>j} 4\epsilon_{ij} \left[ \left( \frac{\sigma_{ij}}{r_{ij}} \right)^{12} - \left( \frac{\sigma_{ij}}{r_{ij}} \right)^6 \right]
 \end{aligned} \tag{1}$$

where the first three terms describe the energy due to stretching, rotation and torsion of the bonds respectively and the last two terms describe the Coulomb and the van der Waals forces.  $\bar{r}$ ,  $\bar{\theta}$  and  $\bar{\omega}$  are the equilibrium bond distances, angles and torsional angles respectively,  $q_i$  are the charges on atoms and  $\epsilon/\sigma$  are the van der Waals constants. For better accuracy, one can augment the force fields with higher order polynomials, such as a cubic term for bond stretching or an exponentially decaying dispersion term. Or one can add many-body terms which describe the secondary effects of two body interactions. However, computing special functions is more expensive than evaluating polynomials and hence classical FFs are usually limited to two-body interaction terms and assume a simple polynomial form for most forces. Apart from the form laid out in Eq. (1), specialized FFs also add additional coordinates to better capture the behavior of a molecular simulation. For example, protein FFs include parameterization in terms of the protein backbone angles, etc. A good force field should reproduce results obtained via known experiments and should be extensible so as to provide useful predictions for other systems.

**Protein force field parameterization.** MD simulations are usually deployed to study protein folding dynamics and to discover stable and metastable conformational states [19]. The accuracy of such MD simulations depend greatly on the quality of chosen force field, which itself depends on the proper parameterization of various constants of the force field. Such parameterization can be done at different levels, such as optimizing the entire force field parameters simultaneously [20, 21] or by focusing on smaller set of parameters (say the torsional terms) while

keeping the rest of the terms fixed [22]. In either case, the MD simulations try to fit the computational results to known reference data. The reference data can be either obtained experimentally or is often generated from high quality *ab initio* simulations. Experimental reference data for such parameterization are expensive to gather and designing proper experiments for novel systems is a non-trivial task. Compared to gathering experimental data, *ab initio* simulations are cheaper to perform and can produce accurate energy surfaces for small molecules to which the force fields might be fitted directly. There is a long history of using *ab initio* quantum chemistry simulations to improve protein force field [23, 24]. In particular, the backbone angle terms of the protein force field are often derived by fitting to the 2-D Ramachandran plot obtained from dipeptide simulations [22, 25]. The ability to perform such dipeptide *ab initio* simulations is hence critical to the task of improving the accuracy of protein force fields [26]. Due to computational complexity of high quality coupled cluster (CC) simulations, current simulations of such dipeptides are often performed at a lower level of theory [27, 28].

*Ab initio* quantum chemistry simulations try to simulate the behavior of a quantum system, viz. a small collection of atoms. Unsurprisingly, the resource requirement to do an exact *ab initio* calculation scales exponentially with the number of atoms in the system. A universal quantum computer can simulate any quantum system with at-most a polynomial overhead [29]. It is then reasonable to argue that a quantum computer which includes quantum effects natively in its hardware should be used to perform such *ab initio* quantum chemistry calculations [30]. In particular, a quantum computer can be used to simulate a molecule’s PES, and hence can be used to perform *ab initio* quantum chemistry calculations. Quantum phase estimation (QPE) can provide comparable accuracy to full configuration interaction (FCI) methods [31] and variational quantum eigensolver (VQE) methods should produce results comparable to coupled cluster theory [32, 33]. As always, care must be taken to translate *ab initio* results obtained in gas phase [34] before they are translated into protein FF parameters which will be applied mostly to aqueous phase.

***Ab initio* Quantum Chemistry on Quantum Computer.** Solving the Schrödinger equation of a molecular Hamiltonian is an especially hard problem. In *ab initio* quantum chemistry methods, this problem is solved iteratively. We build an approximate solution by neglecting some aspect of the Hamiltonian and this solution is used as a starting point for the next iteration where a few more terms of the Hamiltonian are added to the calculation. *Ab initio* methods can be divided into two groups; the Hartree-Fock (HF) method [35] which attempts to find the mean field solution of the problem and post-HF methods which attempt to systematically improve on the HF solution. We describe the details of HF method in Appendix A and focus our discussion on the post-HF

methods. The post-HF methods become particularly easy to analyze in second quantized formulation of the quantum Hamiltonian [36]:

$$\hat{H} = \sum_{ij} h_{ij} a_i^\dagger a_j + \sum_{ijkl} V_{ijkl} a_i^\dagger a_j^\dagger a_l a_k \quad (2)$$

where  $a_i^\dagger$  ( $a_i$ ) are the creation (annihilation) operators that add (remove) an electron to orbital  $i$  and the terms  $h_{ij}$  and  $V_{ijkl}$  describe the kinetic and potential energy of the Hamiltonian. We provide a detailed analysis of the second quantization method in Appendix B.

The coupled cluster (CC) method [37] is one post-HF method which is widely used for computing accurate properties of small molecules. The CC method starts with a reference wave function (usually the HF wave function) that describes a list of orbitals, of which the low energy orbitals are occupied while the high energy orbitals remain empty. The CC method constructs an exponential ansatz (a trial wave function) by exciting some electrons from occupied orbitals to empty orbitals which can be mathematically written as

$$\begin{aligned} |\Psi_{\text{CC}}\rangle &= \exp(\hat{T}_1 + \hat{T}_2 + \dots) |\Psi_{\text{HF}}\rangle, \\ \hat{T}_1 &= \sum_{i,a} t_i^a a_a^\dagger a_i, \\ \hat{T}_2 &= \sum_{ij,ab} t_{ij}^{ab} a_a^\dagger a_b^\dagger a_j a_i, \text{ etc.} \end{aligned} \quad (3)$$

where the indices  $i, j, \dots$  run over the occupied levels,  $a, b, \dots$  run over the unoccupied level and  $|\Psi_{\text{HF}}\rangle$  is the reference wave function obtained from the HF method. Different excitations are given different coefficients ( $t_i^a, t_{ij}^{ab}, \dots$ ) and these coefficients are optimized to give the best solution. The CC equations are usually solved via a projective method (see Appendix C) which does not preserve the variational nature of the ansatz. Thus, the computed energy is no longer an upper bound on the true ground state energy of the system.

The unitary coupled cluster (UCC) method is a modification of the CC method where the ansatz maintains its variational nature. This is achieved by considering both the excitation of electrons from occupied to unoccupied orbitals and their relaxation back to the original orbitals,

$$|\Psi_{\text{UCC}}\rangle = \exp(\hat{T}_1 - \hat{T}_1^\dagger + \hat{T}_2 - \hat{T}_2^\dagger + \dots) |\Psi_{\text{HF}}\rangle \quad (4)$$

This maintains the variational nature of the system as  $\exp(\hat{T} - \hat{T}^\dagger)$  is a unitary operator. The UCC ansatz of Eq. (4) can be efficiently prepared by a quantum computer, and the ground state energy can be found by minimizing the expectation value  $E = \langle \Psi_{\text{UCC}} | H | \Psi_{\text{UCC}} \rangle$ .

In the variational quantum eigensolver (VQE) algorithm, a quantum computer is used to prepare the ansatz and a classical optimizer optimizes the parameters of the ansatz [38–40]. The energy found via the VQE algorithm

remains an upper bound to the true ground state energy of the molecular Hamiltonian and is hopefully more accurate for complex systems. Since the method is variational, an error in preparation of UCC ansatz (Eq. (4)) reflects as a slightly different optimal value of its coefficients. Thus, the VQE method is especially suitable for the noisy computers in the noisy intermediate-scale quantum (NISQ) [41] computing era. As a downside, depending on the PES of the molecule and the quality of the classical optimizer, VQE might take a long time to find the minimum energy or get stuck in a local minima. In general, the VQE algorithm can be used with any ansatz that can be prepared by applying a unitary operator on the reference wave function,

$$|\Psi\rangle = U_{\text{ansatz}} |\Psi_{\text{HF}}\rangle \quad (5)$$

Different types of ansatz might be chosen on the basis of hardware connectivity, the ease of preparation, rate of convergence, etc. Thus, some of the above mentioned downsides may be alleviated by a good choice of ansatz.

On current generation of quantum computers, small molecules such as  $\text{H}_2$  [39, 42, 43],  $\text{HeH}^+$  [38, 44],  $\text{LiH}$  [42] and  $\text{BeH}_2$  [42] have been simulated to good accuracy by utilizing up to six qubits. The VQE algorithm has also been applied to compute the energy of an atomic nucleus [45]. We provide further details of the VQE algorithm in Appendix D.

## Results

**Resource Estimate for FF Parameterization.** Like classical algorithms, it is essential to estimate the resources required for implementing a quantum algorithm. Such estimates help us in understanding the practical application of the given quantum algorithm and guide further optimizations. In quantum computing, the number of qubits and the number of gates are the two physical resources required to implement a quantum algorithm.

A qubit serves as the fundamental unit of information in quantum computing [46]. Classical algorithms are often constrained by the amount of available memory, which is the number of bits required to represent and process the problem. Similarly, quantum algorithms are constrained by the number of qubits required to implement them on a quantum computer. In this aspect, the number of qubits play a role similar to the memory size of a classical computer. Just like a classical computer, the qubits can either hold the information about the problem variable or they might hold temporary or ancillary information required in the course of computation. A qubit can exist as a superposition of state 0 and 1 and can be represented by a two element column vector or in the Dirac’s bra-ket notation [47] as

$$|\psi\rangle = \alpha |0\rangle + \beta |1\rangle \equiv \begin{pmatrix} \alpha \\ \beta \end{pmatrix} \quad (6)$$

Dipeptide	STO-3G	cc-pVDZ	cc-pVTZ(-f)
Alanine	134	428	1598
Arginine	282	904	3374
Asparagine	198	616	2306
Aspartic Acid	194	596	2234
Cysteine	170	500	1846
Glutamine	226	712	2662
Glutamic Acid	222	692	2590
Glycine	106	332	1242
Histidine	242	748	2802
Isoleucine	218	716	2666
Leucine	218	716	2666
Lysine	242	792	2950
Methionine	226	692	2558
Phenylalanine	270	844	3158
Proline	182	580	2166
Serine	154	484	1810
Threonine	182	580	2166
Tryptophan	334	1032	3866
Tyrosine	290	900	3370
Valine	190	620	2310

TABLE I. **Qubit estimation.** The number of qubits required to simulate dipeptides in various basis sets without an active space approximation. All orbitals, including the core orbitals, are included in the VQE computation.

where  $\alpha$  and  $\beta$  are complex numbers. When measured, the qubit in state  $|\psi\rangle$  will report value 1 with probability  $|\alpha|^2$  and the value 0 with probability  $|\beta|^2$ . Since 0 and 1 are the only two possible values, the state  $|\psi\rangle$  must be normalized such that  $|\alpha|^2 + |\beta|^2 = 1$ . Two qubits can be in four possible states, 00, 01, 10 and 11 and can be represented by a 4 element column vector. In general, a  $n$ -qubit state can be represented by  $2^n$  element column vector.

A quantum gate represents an action on the state of one or many quantum qubits. A quantum gate acting on  $n$ -qubits can be represented by a  $2^n \times 2^n$  unitary matrix  $U$

$$U = \begin{pmatrix} u_{11} & u_{12} & \dots & u_{1N} \\ u_{21} & u_{22} & \dots & u_{2N} \\ \vdots & \vdots & \ddots & \vdots \\ u_{N1} & u_{N2} & \dots & u_{NN} \end{pmatrix} \quad (7)$$

where  $N = 2^n$  and  $U^\dagger U = \mathbf{1}_{N \times N}$ . Each quantum gate takes some time to complete its action which is called the gate operation time. If all gates act one after the other, the time required for the quantum algorithm is simply the sum of the operation time of each gate. Quite frequently, a quantum algorithm can split into a series of steps such that gates in each of these steps can be applied simultaneously. The number of such steps is called the circuit depth of the circuit. In this case, the

Dipeptide	$M$	$\eta$
Alanine	112	64
Arginine	236	132
Asparagine	164	96
Aspartic Acid	160	96
Cysteine	128	76
Glutamine	188	108
Glutamic Acid	184	108
Glycine	88	52
Histidine	200	112
Isoleucine	184	100
Leucine	184	100
Lysine	204	112
Methionine	176	100
Phenylalanine	224	120
Proline	152	84
Serine	128	76
Threonine	152	88
Tryptophan	276	148
Tyrosine	240	132
Valine	160	88

TABLE II. **Qubit estimation with active space approximation.** The number of qubits  $M$  required to simulate dipeptides with  $\eta$  valence electrons in with full reaction space approximation. The number of qubits  $M$  are independent of the choice of the basis set, and depend only on the number of valence orbitals of each atom.

time to complete the algorithm is equal to the circuit depth times the operation time of the slowest gate. The circuit depth is a measure of the time complexity of a quantum algorithm, but the number of gates is a good measure of the quantum resource requirement since it dictates the physical complexity of the hardware.

Here, we shall focus on the number of qubits and gates, and circuit depth required to implement quantum *ab initio* simulations for protein force field parameterization.

**Qubit count.** To get a qubit estimate for optimizing protein force-field (FF) parameters, we first start with an estimate for full quantum computation of the electronic wave function of dipeptide molecules. The number of qubits required to simulate a system is double the number of basis functions, one for each spin orbital function (See Methods, [Jordan Wigner transform](#)). The basis functions are chosen from a basis set during the HF optimization. We provide further details of basis sets in the Appendix E. In Table I, we show the number of qubits required to simulate dipeptide molecules in various minimal and split- $\zeta$  basis sets. This is a worse case estimate and the structure of the molecular Hamiltonian can suggest several optimizations that can reduce this resource requirement.

The simplest way to reduce the qubit requirement is to reduce the number of basis functions. Much of the

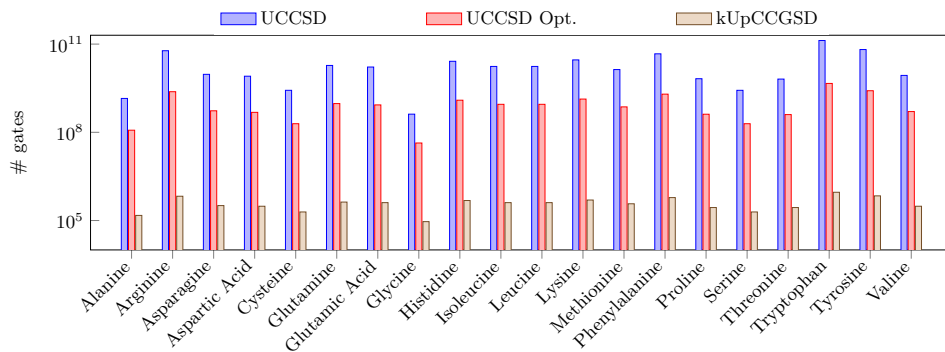


FIG. 1. **Number of two-qubit gates required to implement VQE with different ansatz.** For a molecule of  $\eta$  electrons and  $M$  spin orbitals, the UCCSD ansatz in the JW encoding requires  $O(M(M - \eta)^2\eta^2)$  gates [48]. The bar plot with legend UCCSD shows the number of two-qubit gates required by various dipeptides. However, clever placement of terms can cancel the overhead of JW encoding [49] which reduces the number of gates by  $O(M)$ . We term this as the UCCSD Optimized method. The largest gains are made by switching to a linear scaling ansatz, such as the  $k$ -UpCCGSD [16] ansatz. We show the  $k = 1$  case.

chemical behavior of atoms can be solely attributed to the arrangement of their valence electrons, the inner electrons don't participate in bond formation and high energy orbitals far beyond the molecular energy scale will never be occupied. This leaves the valence orbitals and few virtual orbitals next to the valence orbitals as the only important orbitals for *ab initio* simulations. Such methods, where one only keeps certain orbitals in the post-HF computation, are called active space methods. Different active space methods differ in their choice of such orbitals. The full reaction space [50] or the minimal molecular basis method selects an active space that contains the same number of valence molecular orbitals as one constructed from a minimal atomic basis set. This space contains the bonding, nonbonding and antibonding orbitals of the molecule, and ignore the core orbitals. If the minimal atomic basis set has  $n$  valence functions, then the active space is constructed from  $n$  low energy molecular orbitals. This approximation works reasonably well for post-HF methods that consider configurations representing states excited from the reference states [51, 52]. With this approximation, Table II lists the number of qubits required to simulate various dipeptides on a quantum computer with full reaction space. The number of qubits required for such computation is independent of the chosen basis set and is equal to the number of qubits required by a minimal atomic basis set, but the values of terms in Eq. (2) will depend on the chosen basis set. The active space method greatly reduces the number of qubits required to do useful computation, potentially at the cost of less accurate results. In particular, an active space restricted to full reaction space might not capture dynamical corrections to the HF energy [53, 54].

The qubit requirement can be reduced even without losing any information about the system. This follows from a simple dimensionality analysis argument. Given  $M$  spin orbitals with  $n$  electron, the possible number of valid many-electron configurations scale as  $\sim \binom{M}{n}$  which is

smaller than the dimension of Hilbert space [46] described by  $M$  qubits,  $2^M$ . Thus, the number of qubits  $Q$  required to describe the system satisfy the relationship

$$\binom{M}{n} \leq 2^Q \leq 2^M. \quad (8)$$

Finding the best encoding with such consideration remains an active topic of research [32]. The qubit tapering method [55] utilizes the symmetries of the Hamiltonian to reduce the number of required qubits. Since the number of electrons and the total spin of the molecule is fixed, qubit tapering can always remove 2 qubits. Due to lack of any other spatial symmetry, we were not able to remove any additional qubits. We describe our work in Appendix F.

**Gate count.** The number of gates required to simulate the molecular Hamiltonian via the VQE algorithm depends on the choice of the ansatz. Here we discuss two different ansatz, the UCC Singles & Doubles (UCCSD) and the  $k$ -Unitary paired Coupled Cluster Generalized Singles & Doubles ( $k$ -UpCCGSD) ansatz.

The UCCSD ansatz truncates the UCC ansatz by only keeping the singles and doubles term in Eq. (4),

$$U_{\text{ansatz}} = \exp\left(\hat{T}_1 - \hat{T}_1^\dagger + \hat{T}_2 - \hat{T}_2^\dagger\right). \quad (9)$$

In order to physically realize this many-body unitary operator, we have to break it into one and two body operator. Since the excitation operators do not commute,  $[\hat{T}_i, \hat{T}_j] \neq 0$ , we apply the Trotter-Suzuki (TS) decomposition [56]

$$e^{\sum_i \hat{T}_i - \hat{T}_i^\dagger} = \left(e^{\sum_i (\hat{T}_i - \hat{T}_i^\dagger)/n}\right)^n \approx \left(\prod_i e^{(\hat{T}_i - \hat{T}_i^\dagger)/n}\right)^n \quad (10)$$

to simplify the unitary. The first order TS expansion,  $n = 1$ , suffices for the purpose. Since the individual terms

of  $\hat{T}_1$  and  $\hat{T}_2$  commute with each other, Eq. (10) can be further simplified as

$$U_{\text{ansatz}} = \prod_{i,a} e^{t_i^a a_a^\dagger a_i - \text{h.c.}} \prod_{ij,ab} e^{t_{ij}^{ab} a_a^\dagger a_b^\dagger a_j a_i - \text{h.c.}} \quad (11)$$

where the indices  $i$  and  $j$  run over the  $\eta$  occupied orbitals, and indices  $a$  and  $b$  run over the  $M - \eta$  virtual orbitals. Each of these unitaries can be applied one after the other on a quantum computer. To prepare this ansatz on a quantum computer, we first translate the fermionic operators  $a$  and  $a^\dagger$  to their corresponding Pauli operators that act in the qubit basis. We provide details of such transformation in Methods. From its form in Eq. (11), it becomes evident that the UCCSD ansatz of molecule with  $\eta$  active electrons and  $M$  active orbitals has  $O((M - \eta)^2 \eta^2)$  parameters. In its simplest implementation [48], the common Jordan-Wigner (JW) encoding adds another  $O(M)$  overhead (See Methods, [Standard circuit](#)). Thus, the number of gates required to implement UCCSD ansatz via VQE scales as  $O(M(M - \eta)^2 \eta^2)$ . However, simple optimization via rearrangement of terms can remove the JW overhead which leads to optimal scaling of gates in UCCSD ansatz [49]. In Fig. 1, we show the number of gates required to implement the UCCSD ansatz with and without the JW overhead.

This scaling of the VQE algorithm can be improved by considering other ansatz instead of the UCCSD ansatz. Low depth or linear scaling ansatz can significantly reduce the resource requirement while maintaining a similar level of accuracy [16, 17]. As an example, we consider the  $k$ -UpCCGSD ansatz introduced in Ref. [16] The  $k$ -UpCCGSD ansatz is implemented by the unitary

$$U_{\text{ansatz}} = \prod_{i=1}^k \exp\left(\hat{T}_1^{(i)} + \hat{T}_2^{(i)} - \text{h.c.}\right) \quad (12)$$

where

$$\begin{aligned} \hat{T}_1^{(i)} &= \sum_{p,q=1}^M t_q^{p(i)} a_p^\dagger a_q \\ \hat{T}_2^{(i)} &= \sum_{p,q=1}^{M/2} t_{q\alpha p\beta}^{p\beta(i)} a_{p\alpha}^\dagger a_{p\beta}^\dagger a_{q\beta} a_{q\alpha} \end{aligned} \quad (13)$$

are  $k$  copies of the generalized paired single and doubles excitation operators. In this ansatz, the orbitals are no longer separated into occupied and virtual orbitals, single electron excitations are allowed between any pair of orbitals and double excitations are allowed from one spatial orbital to other. The pairing of electrons for double excitations greatly reduces the number of parameters in the  $k$ -UpCCGSD ansatz which scales as  $O(kM^2)$ . In Fig. 1, we show the number of two-qubit gates required to implement the unitary with  $k = 1$ . As expected, the  $k$ -UpCCGSD ansatz require an order of magnitude fewer gates than the UCCSD ansatz. The parameter  $k$  needs to

Dipeptide	Circuit depth
Alanine	1400
Arginine	2900
Asparagine	2000
Aspartic Acid	1950
Cysteine	1600
Glutamine	2300
Glutamic Acid	2250
Glycine	1100
Histidine	2500
Isoleucine	2250
Leucine	2250
Lysine	2500
Methionine	2150
Phenylalanine	2750
Proline	1850
Serine	1600
Threonine	1900
Tryptophan	3350
Tyrosine	2900
Valine	1950

TABLE III. **Approximate circuit depth to implement  $k$ -UpCCGSD ansatz.** We estimate the approximate circuit depth by scaling gate count by a factor of  $O(M)$  where  $M$  is the number of spin orbitals used to simulate each dipeptide. We show the  $k = 1$  case.

be tuned experimentally. Initial work shows that  $k$  does not scales as fast as  $M$  [16], but more work will be required to find an optimal  $k$  value for dipeptide simulation.

**Circuit Depth.** The circuit depth of these quantum circuits will depend on the number of gates that can be applied simultaneously during preparation of the ansatz. In simplest form, the gates that act on different qubits of a wave function can be applied simultaneously. For example, we can prepare the  $k$ -UpCCGSD ansatz via the circuit denoted by Eq. (11) by simultaneously applying terms with coefficients  $t_{qq}^{pp}$  and  $t_{q'q'}^{p'p'}$  as long as they act on different qubits. If the spin orbitals of the  $k$ -UpCCGSD ansatz are labeled such that consecutive qubits represent the  $\alpha$  and  $\beta$  spin orbitals, then the terms where  $p < p' < q' < q$  can be applied simultaneously. In this case, the term with coefficient  $(p', q')$  is nested inside the term with coefficient  $(p, q)$  and hence can be applied simultaneously [49]. In general, the circuit depth is a factor of  $O(M)$  smaller than the number of gates used to implement the ansatz [16] (See Methods, [Nesting terms](#)). In Table III, we show the approximate circuit depth of the  $k$ -UpCCGSD ansatz implemented for several dipeptide simulations. These circuits have a circuit depth of roughly a few thousands at  $k = 1$ , but practical implementation of these ansatz might require a higher value of  $k$  [16].

## Discussion

Quantum computing holds great promise of improving accuracy and the scale of numerical simulations used in chemistry and other sciences. In particular, quantum computing can enable high quality *ab initio* simulations at a larger scale than possible via current classical computational techniques. An accurate computation via *ab initio* methods remains the only viable tool for quantitative analysis of a system where quantum effects dominate, such as those with few atoms, where bond breaking/formation takes place, etc. At larger scale, MD simulations can provide accurate predictions for chemical reactions, provided one starts with a high quality force field. We have discussed the use of quantum computing and related *ab initio* simulation capabilities to tie these two approaches together, where results from quantum computing simulations can guide the development of better force fields. As an illustrative example, we have provided quantum resource estimates for performing dipeptide simulation, a task of direct importance for optimizing protein force fields. This task requires a few hundred qubits and a circuit depth of few thousands. Current generation of quantum computers, with around 50 qubits and a possible circuit depth of a thousand [57] are only an order of magnitude away from this requirement. Thus, these computations with active space reduction are feasible to attain on the NISQ era quantum computers.

Our work comes with some important caveats. We have assumed that we have access to a quantum computer with all to all qubit connectivity and that these qubits can be controlled via single qubit rotations and CNOT gates. This allows us to assume that we can assign a spin orbital to an arbitrary qubit. However, regular quantum hardware has a connectivity graph with finite degree and additional qubits and gates will be required to overcome this limited connectivity. Ancillary qubits might also be required to perform required quantum gates, further increasing the qubit count. Thus, our work should be taken as a lower bound towards the required quantum resources. Nevertheless, the scaling of the circuit depth and qubit count of an optimal ansatz will remain linear in the size of molecules.

This linear scaling allows us to consider further improvement for protein force field parameterization beyond dipeptide simulations, such as tripeptides simulation [58, 59]. Simulations of larger peptide structure might reveal terms in a protein force field which depend on higher order interaction of peptides. *Ab initio* data can be used to improve other forms of force fields, such as *ab initio* force field (AIFF) [13] and neural network potential (NNP) [14, 15] force field. These ideas serve as future extensions to this work.

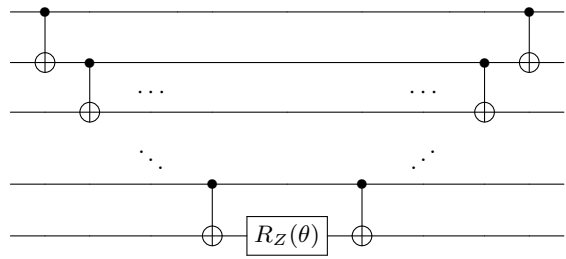


FIG. 2. Quantum circuit that implements the unitary  $\exp(i\theta Z_1 Z_2 \dots Z_n)$

## Methods

**Jordan Wigner transform.** The electronic Hamiltonian, Eq. (2) is written in terms of indistinguishable fermions, while the qubits of a quantum computer are distinct registers with no specific spin. We require a transform that will allow us to represent electronic system on qubits. This task is called encoding, where the fermionic operators are rewritten as a string of operators on qubits. In the JW encoding, each spin orbital is represented by a qubit. If the spin orbital is occupied, the qubit is set to state  $|1\rangle$  and it is set to  $|0\rangle$  otherwise. If the size of our basis set is  $M$ , then we require  $M$  qubits to encode the wave function. The vacuum state  $|\Psi\rangle = |0\rangle$  is represented as  $|\Psi\rangle = |0\rangle^{\otimes M}$  in qubit representation, while state  $|ij\rangle$  with one electron each in orbital  $i$  and  $j$  is written as

$$|\Psi\rangle = |ij\rangle \equiv |000\dots 010\dots 00100\dots 0\rangle \quad (14)$$

where the subscripts denote the index of the orbital in qubit notation. Next, we have to specify the creation  $a_i^\dagger$  and annihilation operators  $a_i$  in terms of single qubit gates. The creation operator should convert qubit  $|0\rangle$  to  $|1\rangle$ , vice-versa for the annihilation operator. They are given by

$$a_i = \sigma_1^z \otimes \sigma_2^z \otimes \dots \otimes \sigma_{i-1}^z \otimes (|0\rangle\langle 1|)_i \quad (15)$$

$$a_i^\dagger = \sigma_1^z \otimes \sigma_2^z \otimes \dots \otimes \sigma_{i-1}^z \otimes (|1\rangle\langle 0|)_i \quad (16)$$

The product of  $\sigma^z$  operator maintains the proper anti-symmetry of the fermionic operators, and is referred to as the JW string. The basis vectors in the JW encoding are simple representation of electron occupation, but fermionic operators become many-qubit gates.

**Standard circuit.** Here, we shall summarize the quantum circuit used by Ref. [48] to implement fermionic operations with JW strings. After JW encoding, various VQE ansatz implement exponentiated strings of Pauli operators, such as a string of  $Z$  operators on  $n$  qubits:

$$U = \exp(i\theta Z_1 Z_2 \dots Z_n) . \quad (17)$$

In Fig. 2, we show the circuit that can implement this unitary only via a basic single qubit gate and CNOT

gates. Pauli strings with other Pauli operators (such as  $X$  or  $Y$ ) can be handled by using the identities

$$\begin{aligned} e^{iX} &= He^{iZ}H \\ e^{iY} &= Ye^{iZ}Y \end{aligned} \quad (18)$$

where  $H$  and  $Y$  are the Hadamard and  $Y$  single qubit gate respectively (See Appendix G). Thus, we can implement all unitaries of exponentiated Pauli strings by combining single qubit gates and the circuit shown in Fig. 2.

**Nesting terms.** In this section, we want to compute the scaling factor between the circuit count and the circuit depth of the  $k$ -UpCCGSD ansatz. The total number of terms in operator  $\hat{T}_2$  of Eq. (13) is  $\frac{M}{2}(\frac{M}{2} - 1)$  and hence the gate count of the circuit scales as  $O(M^2)$ . Two terms  $(p, q)$  and  $(p', q')$  of this operator can be applied

simultaneously if they are nested inside each other such that  $p > p' > q' > q$  [49]. Let  $S(p, q)$  be the set of consecutive terms separated by one spatial orbital that can be nested inside the term  $(p, q)$ , that is,

$$\begin{aligned} S(p, q) &= \{(p, q), (p-1, q+1), (p-2, q+2), \dots\} \\ &\equiv \{(l, m) \mid l+m = p+q, l > m\}. \end{aligned} \quad (19)$$

The number of such distinct disjoint sets is the number of possible values of  $p+q$  where  $p, q \in \{1, 2, 3, \dots, M/2\}$  and  $M$  is the number of distinct spin orbitals. The distinct values of  $p+q$  ranges between 3 to  $M-1$ , and the number of such distinct sets is  $M-3$ . So, the circuit depth of the  $k$ -UpCCGSD ansatz scales as  $O(M)$ , which is an  $O(M)$  improvement over its gate count which scales as  $O(M^2)$ .

**Acknowledgement.** We thanks Shu Ching Ou, Micheal Gilson and Evgeny Epifanovsky for useful discussion.

\* anurag@qulab.com

- [1] M. Levitt and A. Warshel, "Computer simulation of protein folding," *Nature* **253**, 694 (1975).
- [2] A. Warshel and M. Levitt, "Theoretical studies of enzymic reactions: Dielectric, electrostatic and steric stabilization of the carbonium ion in the reaction of lysozyme," *J. Mol. Biol.* **103**, 227–249 (1976).
- [3] J. D. Durrant and J. A. McCammon, "Molecular dynamics simulations and drug discovery," *BMC Biol.* **9**, 71 (2011).
- [4] Y. Guo, C. Riplinger, U. Becker, D. G. Liakos, Y. Minenkov, L. Cavallo, and F. Neese, "Communication: An improved linear scaling perturbative triples correction for the domain based local pair-natural orbital based singles and doubles coupled cluster method [DLPNO-CCSD(T)]," *J. Chem. Phys.* **148**, 011101 (2018).
- [5] C. J. Cramer, *Essentials of Computational Chemistry: Theories and Models*, 2nd ed. (Wiley, 2004).
- [6] L. Wang *et al.*, "Accurate and Reliable Prediction of Relative Ligand Binding Potency in Prospective Drug Discovery by Way of a Modern Free-Energy Calculation Protocol and Force Field," *J. Am. Chem. Soc.* **137**, 2695–2703 (2015).
- [7] C. Chipot and A. Pohorille, eds., *Free Energy Calculations: Theory and Applications in Chemistry and Biology*, Springer Series in Chemical Physics (Springer-Verlag, Berlin Heidelberg, 2007).
- [8] C. D. Snow, H. Nguyen, V. S. Pande, and M. Gruebele, "Absolute comparison of simulated and experimental protein-folding dynamics," *Nature* **420**, 102 (2002).
- [9] R. Chakrabarti, A. M. Klibanov, and R. A. Friesner, "Computational prediction of native protein ligand-binding and enzyme active site sequences," *Proc. Natl. Acad. Sci. USA* **102**, 10153–10158 (2005).
- [10] G. Palermo, C. G. Ricci, and J. A. McCammon, "The invisible dance of CRISPR-Cas9," *Phys. Today* **72**, 30–36 (2019).
- [11] L. Heo and M. Feig, "Experimental accuracy in protein structure refinement via molecular dynamics simulations," *Proc. Natl. Acad. Sci. USA* **115**, 13276–13281 (2018).
- [12] H. Hu and W. Yang, "Free Energies of Chemical Reactions in Solution and in Enzymes with Ab Initio Quantum Mechanics/Molecular Mechanics Methods," *Annu. Rev. Phys. Chem.* **59**, 573–601 (2008).
- [13] P. Xu, E. B. Guidez, C. Bertoni, and M. S. Gordon, "Perspective: Ab initio force field methods derived from quantum mechanics," *J. Chem. Phys.* **148**, 090901 (2018).
- [14] J. S. Smith, O. Isayev, and A. E. Roitberg, "ANI-1: An extensible neural network potential with DFT accuracy at force field computational cost," *Chem. Sci.* **8**, 3192–3203 (2017).
- [15] S. Chmiela, H. E. Sauceda, K.-R. Müller, and A. Tkatchenko, "Towards exact molecular dynamics simulations with machine-learned force fields," *Nat. Commun.* **9**, 3887 (2018).
- [16] J. Lee, W. J. Huggins, M. Head-Gordon, and K. B. Whaley, "Generalized Unitary Coupled Cluster Wave functions for Quantum Computation," *J. Chem. Theory Comput.* **15**, 311–324 (2019), [arXiv:1810.02327](https://arxiv.org/abs/1810.02327).
- [17] I. D. Kivlichan, J. McClean, N. Wiebe, C. Gidney, A. Aspuru-Guzik, G. K.-L. Chan, and R. Babbush, "Quantum Simulation of Electronic Structure with Linear Depth and Connectivity," *Phys. Rev. Lett.* **120**, 110501 (2018).
- [18] A. R. Leach, *Molecular Modelling: Principles and Applications* (Prentice Hall, 2001).
- [19] J. Lee, P. L. Freddolino, and Y. Zhang, "Ab Initio Protein Structure Prediction," in *From Protein Structure to Function with Bioinformatics*, edited by D. J. Rigden (Springer Netherlands, Dordrecht, 2017) pp. 3–35.
- [20] L.-P. Wang, T. J. Martinez, and V. S. Pande, "Building Force Fields: An Automatic, Systematic, and Reproducible Approach," *J. Phys. Chem. Lett.* **5**, 1885–1891 (2014).
- [21] P. Robustelli, S. Piana, and D. E. Shaw, "Developing a molecular dynamics force field for both folded and disordered protein states," *Proc. Natl. Acad. Sci. USA* **115**, E4758–E4766 (2018).
- [22] R. B. Best, X. Zhu, J. Shim, P. E. M. Lopes, J. Mittal, M. Feig, and A. D. MacKerell, "Optimization of the Additive CHARMM All-Atom Protein Force Field Targeting



- Improved Sampling of the Backbone  $\phi$ ,  $\psi$  and Side-Chain X1 and X2 Dihedral Angles,” *J. Chem. Theory Comput.* **8**, 3257–3273 (2012).
- [23] J. W. Ponder and D. A. Case, “Force Fields for Protein Simulations,” in *Advances in Protein Chemistry*, Protein Simulations, Vol. 66 (Academic Press, 2003) pp. 27–85.
- [24] P. E. M. Lopes, O. Guvench, and A. D. MacKerell, “Current Status of Protein Force Fields for Molecular Dynamics Simulations,” in *Molecular Modeling of Proteins*, Methods in Molecular Biology, edited by A. Kukol (Springer New York, New York, NY, 2015) pp. 47–71.
- [25] G. A. Kaminski, H. A. Stern, B. J. Berne, R. A. Friesner, Y. X. Cao, R. B. Murphy, R. Zhou, and T. A. Halgren, “Development of a polarizable force field for proteins via ab initio quantum chemistry: First generation model and gas phase tests,” *J. Comput. Chem.* **23**, 1515–1531 (2002).
- [26] J. Hermans, “The amino acid dipeptide: Small but still influential after 50 years,” *Proc. Natl. Acad. Sci. USA* **108**, 3095–3096 (2011).
- [27] P. Echenique and J. L. Alonso, “Efficient model chemistries for peptides. I. General framework and a study of the heterolevel approximation in RHF and MP2 with Pople split-valence basis sets,” *J. Comput. Chem.* **29**, 1408–1422 (2008).
- [28] V. Mironov, Y. Alexeev, V. K. Mulligan, and D. G. Fedorov, “A systematic study of minima in alanine dipeptide,” *J. Comput. Chem.* **40**, 297–309 (2019).
- [29] S. Lloyd, “Universal Quantum Simulators,” *Science* **273**, 1073–1078 (1996).
- [30] R. P. Feynman, “Simulating physics with computers,” *Int. J. Theor. Phys.* **21**, 467–488 (1982).
- [31] D. S. Abrams and S. Lloyd, “Quantum Algorithm Providing Exponential Speed Increase for Finding Eigenvalues and Eigenvectors,” *Phys. Rev. Lett.* **83**, 5162–5165 (1999), [arXiv:quant-ph/9807070](#).
- [32] T. Takeshita, N. C. Rubin, Z. Jiang, E. Lee, R. Babbush, and J. R. McClean, “Increasing the representation accuracy of quantum simulations of chemistry without extra quantum resources,” [arXiv Preprint \(2019\)](#), [arXiv:1902.10679](#).
- [33] M. Kühn, S. Zanker, P. Deglmann, M. Marthaler, and H. Weiß, “Accuracy and Resource Estimations for Quantum Chemistry on a Near-Term Quantum Computer,” *J. Chem. Theory Comput.* **15**, 4764–4780 (2019), [arXiv:1812.06814](#).
- [34] R. C. Rizzo and W. L. Jorgensen, “OPLS All-Atom Model for Amines: Resolution of the Amine Hydration Problem,” *J. Am. Chem. Soc.* **121**, 4827–4836 (1999).
- [35] D. R. Hartree, “The Wave Mechanics of an Atom with a Non-Coulomb Central Field. Part I. Theory and Methods,” *Math. Proc. Cambridge Philos. Soc.* **24**, 89–110 (1928); “The Wave Mechanics of an Atom with a Non-Coulomb Central Field. Part II. Some Results and Discussion,” *Math. Proc. Cambridge Philos. Soc.* **24**, 111–132 (1928); V. Fock, “Näherungsmethode zur Lösung des quantenmechanischen Mehrkörperproblems,” *Z. Physik* **61**, 126–148 (1930); J. C. Slater, “Note on Hartree’s Method,” *Phys. Rev.* **35**, 210–211 (1930).
- [36] T. Helgaker, P. Jorgensen, and J. Olsen, *Molecular Electronic-Structure Theory* (John Wiley & Sons, 2014).
- [37] R. J. Bartlett and M. Musiał, “Coupled-cluster theory in quantum chemistry,” *Rev. Mod. Phys.* **79**, 291–352 (2007).
- [38] A. Peruzzo, J. McClean, P. Shadbolt, M.-H. Yung, X.-Q. Zhou, P. J. Love, A. Aspuru-Guzik, and J. L. O’Brien, “A variational eigenvalue solver on a photonic quantum processor,” *Nat. Commun.* **5**, 4213 (2014).
- [39] P. J. J. O’Malley *et al.*, “Scalable Quantum Simulation of Molecular Energies,” *Phys. Rev. X* **6**, 031007 (2016).
- [40] J. R. McClean, J. Romero, R. Babbush, and A. Aspuru-Guzik, “The theory of variational hybrid quantum-classical algorithms,” *New J. Phys.* **18**, 023023 (2016).
- [41] J. Preskill, “Quantum Computing in the NISQ era and beyond,” *Quantum* **2**, 79 (2018), [arXiv:1801.00862](#).
- [42] A. Kandala, A. Mezzacapo, K. Temme, M. Takita, M. Brink, J. M. Chow, and J. M. Gambetta, “Hardware-efficient variational quantum eigensolver for small molecules and quantum magnets,” *Nature* **549**, 242–246 (2017), [arXiv:1704.05018](#).
- [43] C. Hempel *et al.*, “Quantum Chemistry Calculations on a Trapped-Ion Quantum Simulator,” *Phys. Rev. X* **8**, 031022 (2018), [arXiv:1803.10238](#).
- [44] Y. Shen, X. Zhang, S. Zhang, J.-N. Zhang, M.-H. Yung, and K. Kim, “Quantum implementation of the unitary coupled cluster for simulating molecular electronic structure,” *Phys. Rev. A* **95**, 020501 (2017), [arXiv:1506.00443](#).
- [45] E. F. Dumitrescu, A. J. McCaskey, G. Hagen, G. R. Jansen, T. D. Morris, T. Papenbrock, R. C. Pooser, D. J. Dean, and P. Lougovski, “Cloud Quantum Computing of an Atomic Nucleus,” *Phys. Rev. Lett.* **120**, 210501 (2018), [arXiv:1801.03897](#).
- [46] M. A. Nielsen and I. L. Chuang, *Quantum Computation and Quantum Information* (Cambridge University Press, 2000).
- [47] P. A. M. Dirac, *The Principles of Quantum Mechanics*, fourth revised ed. (Clarendon Press, 1981).
- [48] J. D. Whitfield, J. Biamonte, and A. Aspuru-Guzik, “Simulation of electronic structure Hamiltonians using quantum computers,” *Mol. Phys.* **109**, 735–750 (2011), [arXiv:1001.3855](#).
- [49] M. B. Hastings, D. Wecker, B. Bauer, and M. Troyer, “Improving Quantum Algorithms for Quantum Chemistry,” *Quantum Inf. Comput.* **15**, 1–21 (2015), [arXiv:1403.1539](#).
- [50] K. Ruedenberg, M. W. Schmidt, M. M. Gilbert, and S. T. Elbert, “Are atoms intrinsic to molecular electronic wavefunctions? I. The FORS model,” *Chem. Phys.* **71**, 41–49 (1982).
- [51] J. Townsend, J. K. Kirkland, and K. D. Vogiatzis, “Post-Hartree-Fock methods: Configuration interaction, many-body perturbation theory, coupled-cluster theory,” in *Mathematical Physics in Theoretical Chemistry*, Developments in Physical & Theoretical Chemistry, edited by S. M. Blinder and J. E. House (Elsevier, 2019) pp. 63–117.
- [52] K. Kowalski, S. Hirata, M. Włoch, P. Piecuch, and T. L. Windus, “Active-space coupled-cluster study of electronic states of Be3,” *J. Chem. Phys.* **123**, 074319 (2005).
- [53] D. K. W. Mok, R. Neumann, and N. C. Handy, “Dynamical and Nondynamical Correlation,” *J. Phys. Chem.* **100**, 6225–6230 (1996).
- [54] A. I. Krylov, C. D. Sherrill, E. F. C. Byrd, and M. Head-Gordon, “Size-consistent wave functions for nondynamical correlation energy: The valence active space optimized orbital coupled-cluster doubles model,” *J. Chem. Phys.* **109**, 10669–10678 (1998).
- [55] S. Bravyi, J. M. Gambetta, A. Mezzacapo, and K. Temme, “Tapering off qubits to simulate fermionic Hamiltonians,” [arXiv Preprint \(2017\)](#), [arXiv:1701.08213 \[quant-ph\]](#).
- [56] D. Poulin, M. B. Hastings, D. Wecker, N. Wiebe, A. C.

- Doherty, and M. Troyer, “The Trotter Step Size Required for Accurate Quantum Simulation of Quantum Chemistry,” [arXiv Preprint \(2014\)](#), [arXiv:1406.4920](#).
- [57] F. Arute *et al.*, “Quantum supremacy using a programmable superconducting processor,” *Nature* **574**, 505–510 (2019).
- [58] S. Anishetty, G. Pennathur, and R. Anishetty, “Tripeptide analysis of protein structures,” *BMC Struct. Biol.* **2**, 9 (2002).
- [59] M. Culka, J. Galgonek, J. Vymětal, J. Vondrášek, and L. Rulíšek, “Toward Ab Initio Protein Folding: Inherent Secondary Structure Propensity of Short Peptides from the Bioinformatics and Quantum-Chemical Perspective,” *J. Phys. Chem. B* **123**, 1215–1227 (2019).
- [60] M. Eichler, “A new proof of the Baker-Campbell-Hausdorff formula,” *J. Math. Soc. Japan* **20**, 23–25 (1968).
- [61] M. R. Hoffmann and J. Simons, “A unitary multiconfigurational coupled-cluster method: Theory and applications,” *J. Chem. Phys.* **88**, 993–1002 (1988).
- [62] Q. Sun *et al.*, “PySCF: The Python-based simulations of chemistry framework,” *Wiley Interdiscip. Rev. Comput. Mol. Sci.* **8**, e1340 (2018).
- [63] W. J. Hehre, R. F. Stewart, and J. A. Pople, “Self-Consistent Molecular-Orbital Methods. I. Use of Gaussian Expansions of Slater-Type Atomic Orbitals,” *J. Chem. Phys.* **51**, 2657–2664 (1969).
- [64] T. H. Dunning, “Gaussian basis sets for use in correlated molecular calculations. I. The atoms boron through neon and hydrogen,” *J. Chem. Phys.* **90**, 1007–1023 (1989).
- [65] S. B. Bravyi and A. Y. Kitaev, “Fermionic Quantum Computation,” *Ann. Phys.* **298**, 210–226 (2002), [arXiv:quant-ph/0003137](#).
- [66] D. Gottesman, *Stabilizer Codes and Quantum Error Correction*, Ph.D., California Institute of Technology, Pasadena (1997), [arXiv:quant-ph/9705052](#).
- [67] D. A. Lidar and T. A. Brun, *Quantum Error Correction* (Cambridge University Press, 2013).
- [68] S. Kim *et al.*, “PubChem 2019 update: Improved access to chemical data,” *Nucleic Acids Res.* **47**, D1102–D1109 (2019).
- [69] G. H. Low *et al.*, “Q# and NWChem: Tools for Scalable Quantum Chemistry on Quantum Computers,” [arXiv Preprint \(2019\)](#), [arXiv:1904.01131](#).

## A. Hartree-Fock theory

In principle, all the properties of a molecular system can be obtained from its wave function which itself can be obtained by solving the Schrödinger equation. Since electrons are much lighter than atomic nuclei, the Born-Oppenheimer approximation neglects the motion of the nuclei. After applying the approximation, the electronic Hamiltonian is given by the sum of electronic kinetic energy and the electron-electron and nuclei-electron

Coulomb interaction energy;

$$H(\{\mathbf{r}_i\}) = -\frac{1}{2} \sum_{i=1}^n \nabla_i^2 + \sum_{i>j}^n \frac{1}{|\mathbf{r}_i - \mathbf{r}_j|} - \sum_{i=1}^n \sum_{\alpha=1}^{N_n} \frac{Z_\alpha}{|\mathbf{r}_i - \mathbf{r}_\alpha|} \quad (\text{A1})$$

where  $n/N_n$  is the number of electrons/nuclei in the molecule,  $\mathbf{r}_i/\mathbf{r}_\alpha$  are the electronic/nuclear coordinates and  $Z_\alpha$  are the nuclear charges. The eigenfunctions to this Hamiltonian are the molecular electronic wave-function of the ground state and various excited states, and the eigenvalues are the corresponding energies. The ground state energy as a function of electronic coordinates,  $E(\{\mathbf{r}_i\})$ , is called the potential energy surface (PES) of the molecule. In general, one cannot find an analytical solution to a many body Schrödinger equation. However, approximate computational methods can yield results which are within computational accuracy.

Let  $\{\phi_j(\mathbf{r})\}$  be a complete basis set such that the wave function of the  $i^{\text{th}}$  electron can be written as

$$\psi_i(\mathbf{r}) = \sum_j c_{ij} \phi_j(\mathbf{r}) \quad (\text{A2})$$

where  $C = [c_{ij}]$  are appropriate coefficients. The possible many-electron states can be constructed from these single electron wave functions. Since electrons are fermions, the many-electron state must be antisymmetric in any two electron coordinates. A many-electron state where the electrons occupy states  $\{\psi_{i_1}, \psi_{i_2}, \dots, \psi_{i_n}\}$  can be written as a Slater’s determinant

$$\Psi(\mathbf{R}, C) = \begin{vmatrix} \psi_{i_1}(\mathbf{r}_1) & \psi_{i_1}(\mathbf{r}_2) & \dots & \psi_{i_1}(\mathbf{r}_n) \\ \psi_{i_2}(\mathbf{r}_1) & \psi_{i_2}(\mathbf{r}_2) & \dots & \psi_{i_2}(\mathbf{r}_n) \\ \vdots & \vdots & \ddots & \vdots \\ \psi_{i_n}(\mathbf{r}_1) & \psi_{i_n}(\mathbf{r}_2) & \dots & \psi_{i_n}(\mathbf{r}_n) \end{vmatrix} \quad (\text{A3})$$

where  $\mathbf{R} = \{\mathbf{r}_1, \mathbf{r}_2, \dots, \mathbf{r}_n\}$  represent the coordinates of the electrons. Note that this state depends on the coefficient matrix  $C$ . In general, the actual electronic wave function can be written as an appropriately weighted sum of these determinants. The Hartree-Fock (HF) approximation assumes that the wave function consists of only one such determinant, and then optimizes the parameters  $C$  of the determinant by applying the variational principle. We want to find the optimal matrix  $C$  that minimizes the expectation energy of the state  $\Psi(\mathbf{R}, C)$  while ensuring that the molecular orbital (MO)  $\psi_i$  are appropriately normalized. We can do this by introducing a set of Lagrange multiplier  $\epsilon_i$  such that

$$\delta \left[ \int \Psi^* H \Psi \, d\mathbf{R} - \sum_i \epsilon_i \int |\psi_i|^2 \, d\mathbf{r}_i \right] = 0 \quad (\text{A4})$$

This leads to a set of single-electron coupled equations, collectively called the Hartree-Fock equations:

$$\left[ -\frac{1}{2}\nabla_i^2 - \sum_{\alpha} \frac{Z_{\alpha}}{|\mathbf{r}_i - \mathbf{r}_{\alpha}|} \right] \psi_i(\mathbf{r}_i) + \sum_{j \neq i} \left[ \int d\mathbf{r}_j \frac{|\psi_j(\mathbf{r}_j)|^2}{|\mathbf{r}_i - \mathbf{r}_j|} \right] \psi_i(\mathbf{r}_i) - \sum_{j \neq i} \left[ \int d\mathbf{r}_j \frac{\psi_j(\mathbf{r}_j)\psi_i(\mathbf{r}_i)}{|\mathbf{r}_i - \mathbf{r}_j|} \right] \psi_i(\mathbf{r}_i) = \epsilon_i \psi_i(\mathbf{r}_i) \quad (\text{A5})$$

The first term on the left hand side is the sum of electron kinetic energy and electron-nuclei Coulomb interaction, the second term is the electronic interaction of electron  $i$  with the mean field electric force of all other electrons and the third term is the exchange energy term. Electrons of the same spin avoid each other due to Pauli's exclusion principle and experience smaller Coulomb repulsion. This gives rise to the exchange energy term.

The HF equations (A5) are highly non-linear as  $\psi_i$  features on both sides of equality. The HF equations are mean-field single electron equations and require the wave functions of all other electrons to write down the Coulomb and exchange energy. The self consistent field (SCF) method is often used to solve these equations. The SCF method starts with a reasonable guess of the single electron wave function, and solves the HF equations assuming the guess wave function for all the other electrons. This solution is then used as the wave function of other electrons, and the HF equations are solved again, yielding a hopefully better wave function. At each step, we keep track of the energy of the solution,  $E = \sum_i \epsilon_i$ . The SCF method stops when the energy converges.

## B. Second Quantization

The HF wave function is a mean-field approximation of the ground state many-body electronic wave function. Since it is constructed from a single determinant, it ignores static and dynamic electron-electron interaction. Post HF methods try to recover this correlation by considering additional electronic configurations. These methods becomes considerably easier to analyze in the second quantization formulation of the Hamiltonian problem. In this section, we describe the method of obtaining second quantized Hamiltonian from variationally optimized HF functions.

We start with the variationally optimized HF molecule orbitals,  $\{\psi_i\}$ , and represent the Slater determinant (A3) in the Dirac notation as

$$|\Psi\rangle \equiv |i_1 i_2 \dots i_n\rangle \quad (\text{B1})$$

This is a  $n$ -electron state, where the electrons occupy the orbitals  $\{i_1, i_2, \dots, i_n\}$  while the other molecular orbitals are empty. In this notation  $|\cdot\rangle$  denotes the state of no electron. The excitation operator  $a_i^\dagger$  creates an electron in one of the orbital:

$$|i j_1 j_2 \dots\rangle = a_i^\dagger |j_1 j_2 \dots\rangle \quad (\text{B2})$$

If state  $i$  is already occupied,  $a_i^\dagger |\Psi\rangle = 0$ . Any state  $|\Psi\rangle$  can be uniquely specified by a string of creation operators,

$$|\Psi\rangle = a_{i_1}^\dagger a_{i_2}^\dagger \dots a_{i_n}^\dagger |0\rangle \quad (\text{B3})$$

Similarly, the annihilation operator  $a_i$  destroys the electron in one of the orbital:

$$|j_1 j_2 \dots\rangle = a_i |i j_1 j_2 \dots\rangle \quad (\text{B4})$$

If the state  $i$  is already unoccupied, then  $a_i |\Psi\rangle = 0$ . These definitions, along with the completely antisymmetric nature of the wave function  $|\Psi\rangle$  imply that these operators obey the canonical anticommutation relationship,

$$\{a_i^\dagger, a_j\} = a_i^\dagger a_j + a_j a_i^\dagger = 0 \quad (\text{B5})$$

$$\{a_i, a_j\} = \{a_i^\dagger, a_j^\dagger\} = 0 \quad (\text{B6})$$

We can now rewrite the Hamiltonian in its second quantized form:

$$\hat{H} = \sum_{ij} h_{ij} a_i^\dagger a_j + \sum_{ijkl} V_{ijkl} a_i^\dagger a_j^\dagger a_l a_k \quad (\text{B7})$$

where

$$h_{ij} = \int \psi_i^*(\mathbf{r}) \left[ -\frac{1}{2}\nabla^2 - \sum_{\alpha} \frac{Z_{\alpha}}{|\mathbf{r} - \mathbf{r}_{\alpha}|} \right] \psi_j(\mathbf{r}) d\mathbf{r}, \quad (\text{B8})$$

$$V_{ijkl} = \int \psi_i^*(\mathbf{r}_1) \psi_j^*(\mathbf{r}_2) \frac{1}{|\mathbf{r}_1 - \mathbf{r}_2|} \psi_k(\mathbf{r}_2) \psi_l(\mathbf{r}_1) d\mathbf{r}_1 d\mathbf{r}_2. \quad (\text{B9})$$

In the limit where the MOs  $\{\psi_i\}$  form a complete basis set, the second quantized representation is exact. In computational chemistry applications, frequently the basis set is limited to  $M$  functions, in which case second quantized Hamiltonian (B7) is only an approximate representation of the electronic Hamiltonian (A1). The Hamiltonian contains  $\mathcal{O}(M^4)$  terms, and becomes increasing hard to solve via exact diagonalization.

## C. Post-Hartree Fock methods

The HF solution serves as a good starting point for post-HF methods, which iterate over the HF solution and show better agreement with experimental results. In this section, we discuss two such post-Hartree Fock methods.

**Configuration interaction method.** A general solution of the full Hamiltonian (A1) can be constructed by taking an appropriate weighted sum of all possible determinants. This is known as the full configuration interaction (FCI) method where the wave function is given by

$$|\Psi_{\text{FCI}}\rangle = \sum c_i |\Psi_i\rangle \quad (\text{C1})$$

The sum is done over all possible determinants of form given by Eq. (A3). If these determinants are constructed out of  $M$  molecular orbitals with  $N$  electrons, the number of possible determinants is  $\binom{M}{N} = \frac{M!}{(M-N)!N!}$  which scales exponentially in  $M$ . Thus, an FCI calculation is intractable except for very small molecules.

The FCI calculation can be simplified by using additional symmetries of the molecule. Hamiltonian (A1) commutes with the spin operators  $\hat{S}_z$  and  $\hat{S}^2$  and also commutes with the z-component of the total angular momentum  $\hat{L}_z$ , that is, the Hamiltonian preserves the total intrinsic spin of electrons and the z-component of the total angular momentum. Thus, the valid determinants in Eq. (C1) should be of same spin. Such a combination of the determinants is called a configuration state function (CSF). Using a CSF can greatly reduce the number of determinants required to construct an FCI wave function. Nevertheless, the number of determinants in CSF wave function also grow exponentially in the size of basis set, and FCI with such methods becomes intractable for large molecules.

In second quantization formulation, the FCI wave function can be constructed systematically from the HF state. Let  $|\Psi_{\text{HF}}\rangle$  be the HF determinant (A3) constructed from molecular orbitals found via the SCF method. The FCI wave function is constructed via a series of excitation operators:

$$|\Psi_{\text{FCI}}\rangle = \left( \sum_{ia} c_i^a a_a^\dagger a_i + \sum_{ij,ab} c_{ij}^{ab} a_a^\dagger a_b^\dagger a_j a_i + \dots \right) |\Psi_{\text{HF}}\rangle \quad (\text{C2})$$

where the indices  $\{i, j, \dots\}$  and  $\{a, b, \dots\}$  run over the occupied and unoccupied orbitals respectively in the  $|\Psi_{\text{HF}}\rangle$  wave function. The different determinants in the FCI expansion are classified as singles (S), doubles (D), triples (T), etc depending on their level of excitation from the HF wave function. The FCI wave function can be systematically approximated via the configuration interaction (CI) method by inclusion of different levels of excitations, for example, CI Singles Doubles (CISD) keeps singles and doubles, CISDTQ also adds triple and quadruple excitations, etc.

**Coupled cluster method.** The CI formulation is exact under the complete basis set limit (i.e.  $M \rightarrow \infty$ ), but is not size extensive and converges very slowly to the full wave function. These shortcomings can be overcome by the coupled cluster (CC) method. The CC wave function is given by

$$|\Psi_{\text{CC}}\rangle = \exp \left( \sum_{i,a} t_i^a a_a^\dagger a_i + \sum_{ij,ab} t_{ij}^{ab} a_a^\dagger a_b^\dagger a_j a_i + \dots \right) |\Psi_{\text{HF}}\rangle \quad (\text{C3})$$

where the indices  $i, j, \dots$  run over the occupied levels and  $a, b, \dots$  run over the unoccupied level. If all excitation levels are included, then the CC and FCI expansions describe

the same wave function. For example, by expanding and comparing the terms in Eqs. (C2) and (C3), we find that

$$c_i^a = t_i^a, \quad (\text{C4})$$

$$c_{ij}^{ab} = t_{ij}^{ab} + \frac{1}{2}(t_i^a t_j^b + t_j^a t_i^b), \quad (\text{C5})$$

etc. The CC wave function is size extensive and usually converges faster than the CI wave function [37].

We want to solve the CC Schrödinger equation  $\hat{H}|\Psi_{\text{CC}}\rangle = E|\Psi_{\text{CC}}\rangle$ . We define the coupled cluster operator

$$\hat{T} = \hat{T}_1 + \hat{T}_2 + \dots \quad (\text{C6})$$

$$= \sum_{i,a} t_i^a a_a^\dagger a_i + \sum_{ij,ab} t_{ij}^{ab} a_a^\dagger a_b^\dagger a_j a_i + \dots \quad (\text{C7})$$

such that

$$|\Psi_{\text{CC}}\rangle = e^{\hat{T}} |\Phi_0\rangle \quad (\text{C8})$$

where  $|\Phi_0\rangle$  is the starting wave function, usually a HF wave function or a CSF. We want to solve for the energy  $E$  and the amplitudes  $\{t_i^a, t_{ij}^{ab}, \dots\}$ . Noting that the determinants  $|\Phi_{ij\dots}^{ab\dots}\rangle = a_a^\dagger a_b^\dagger \dots a_j a_i |\Phi_0\rangle$  form an orthonormal set, we can write down the coupled cluster equations:

$$\langle \Phi_0 | e^{-\hat{T}} \hat{H} e^{\hat{T}} | \Phi_0 \rangle = E \quad (\text{C9})$$

$$\langle \Phi_{ij\dots}^{ab\dots} | e^{-\hat{T}} \hat{H} e^{\hat{T}} | \Phi_0 \rangle = 0 \quad (\text{C10})$$

The operator  $e^{-\hat{T}} \hat{H} e^{\hat{T}}$  can be simplified via the Baker-Campbell-Hausdorff (BCH) expansion [60] and by noting that this series terminates because the Hamiltonian  $\hat{H}$  as written in Eq. (B7) only contains 2-excitation operators. Thus,

$$\begin{aligned} e^{-\hat{T}} \hat{H} e^{\hat{T}} &= \hat{H} + [\hat{H}, \hat{T}] + \frac{1}{2!} [\hat{H}, [\hat{H}, \hat{T}]] + \frac{1}{3!} [\hat{H}, [\hat{H}, [\hat{H}, \hat{T}]]] \\ &\quad + \frac{1}{4!} [\hat{H}, [\hat{H}, [\hat{H}, [\hat{H}, \hat{T}]]]] \end{aligned} \quad (\text{C11})$$

The above technique describes a projective method of solving the CC equations. The projective CC equations are convenient to solve via numerical methods. The energy formula in Eq. (C9) does not conform to variational condition as the operator  $e^{-\hat{T}} \hat{H} e^{\hat{T}}$  is not Hermitian. Thus, energy found via solving Eq. (C9) with a truncated operator  $\hat{T}$  might not be an upper bound to the true coupled cluster energy. We can construct a variational solution by starting from Eqs. (C6) and (C8) and using the Hermitian conjugate of  $e^{\hat{T}}$ . This yields a variational form such that for truncated operator  $\hat{\tau} = \sum_i^n T_i$ ,

$$E = \frac{\langle \Phi_0 | (e^{\hat{T}})^\dagger \hat{H} e^{\hat{T}} | \Phi_0 \rangle}{\langle \Phi_0 | (e^{\hat{T}})^\dagger e^{\hat{T}} | \Phi_0 \rangle} \leq \tilde{E} = \frac{\langle \Phi_0 | (e^{\hat{\tau}})^\dagger \hat{H} e^{\hat{\tau}} | \Phi_0 \rangle}{\langle \Phi_0 | (e^{\hat{\tau}})^\dagger e^{\hat{\tau}} | \Phi_0 \rangle}. \quad (\text{C12})$$

The operator  $(e^{\hat{\tau}})^\dagger \hat{H} e^{\hat{\tau}}$  does not have a known finite length expansion which makes finding solutions of Eq. (C12) a considerably harder computational task when compared to the projective methods. Nevertheless, it can be approximated by expanding  $e^{\hat{\tau}}$  via a Taylor series and then truncating it. Such truncation is arbitrary and leads to additional errors.

A similar variational method called the unitary coupled cluster (UCC) method tries a different approach. The cluster operator  $\hat{T}$  is replaced by an anti-Hermitian operator  $\hat{T} - \hat{T}^\dagger$  such that  $\hat{U} = e^{\hat{T} - \hat{T}^\dagger}$  is a unitary operator. The resultant operator  $\hat{U}^\dagger \hat{H} \hat{U}$  in

$$E = \langle \Phi_0 | \hat{U}^\dagger \hat{H} \hat{U} | \Phi_0 \rangle \quad (\text{C13})$$

can be thought as a rotation of basis such that  $\hat{H}' = \hat{U}^\dagger \hat{H} \hat{U}$  is a Hamiltonian that has the same eigenvalues as  $\hat{H}$ . A systematic series expansion of  $\hat{H}'$  can be obtained where we truncate the series by keeping all terms to a particular order of perturbation theory [61]. Alternatively, the energy  $E = \langle \Phi' | \hat{H} | \Phi' \rangle$  can be thought as the expectation value of the Hamiltonian with respect to the wave function

$$|\Phi'\rangle = \hat{U} |\Phi_0\rangle \quad (\text{C14})$$

This approach is suitable to quantum computing where a universal quantum computer can efficiently prepare the state  $|\Phi'\rangle$  by applying the unitary  $\hat{U}$  on an initial state  $|\Phi_0\rangle$ .

#### D. Variational quantum eigensolver

The variational quantum eigensolver (VQE) method repeatedly prepares a variational quantum state  $|\Psi(\mathbf{t})\rangle$  and optimizes over the unknown parameters  $\mathbf{t}$  to estimate the ground state energy. A quantum computer can be used to efficiently prepare the state  $|\Psi(\mathbf{t})\rangle$  and the energy of this state  $E(\mathbf{t}) = \langle \Psi(\mathbf{t}) | H | \Psi(\mathbf{t}) \rangle$  can be estimated on a classical computer via repeated measurements of the quantum state. A classical optimizer optimizes the parameters  $\mathbf{t}$  to minimize energy  $E(\mathbf{t})$ . Thus, VQE is a hybrid classical-quantum algorithm.

Different encoding methods convert the fermionic Hamiltonian to a qubit-based Hamiltonian which is a weighted sum of strings of Pauli operators,

$$H = \sum_i H_i \prod_{\sigma_i} \sigma_j^\alpha \quad (\text{D1})$$

where  $\alpha \in \{x, y, z\}$  specifies one of the Pauli operators and  $\sigma_j^\alpha \in \sigma_i$  where  $\sigma_i$  is a set of Pauli operators describing the Pauli string of  $i^{\text{th}}$  term. The parameters  $H_i$  depend on the parameters  $h_{ij}$  and  $V_{ijkl}$  computed via Eqs. (B8) and (B9) and can be calculated with a quantum chemistry package such as PySCF [62]. With an initial guess for  $\mathbf{t}$ , we construct a quantum circuit that implements the unitary

$U_{\text{ansatz}}(\mathbf{t})$ . The qubits are initialized in the reference state  $|\Phi_0\rangle$  and the quantum circuit then prepares  $|\Psi(\mathbf{t})\rangle$ . The energy of this state is found via repeated preparation of state  $|\Psi(\mathbf{t})\rangle$  followed by local measurements. The energy is given by

$$E(\mathbf{t}) = \sum_i H_i \prod_{\bar{\sigma}} \langle \Psi(\mathbf{t}) | \sigma_j^\alpha | \Psi(\mathbf{t}) \rangle \quad (\text{D2})$$

The parameters  $\mathbf{t}$  are then optimized to obtain the best estimate of the ground state energy. This optimization is done via a classical algorithm, such as gradient descent, and hence VQE is a hybrid classical-quantum algorithm. At each step of optimization, the parameters  $\mathbf{t}$  are suitably changed to  $\bar{\mathbf{t}}$  to prepare a new state  $|\Psi(\bar{\mathbf{t}})\rangle$  and this process is repeated till the energy  $E$  converges to a stable value.

Application of the variational principle requires an ansatz which has large overlap with the ground state wave function. The UCC and  $k$ -Unitary paired Coupled Cluster Generalized Singles & Doubles ( $k$ -UpCCGSD) methods construct their ansatz in a chemically intuitive way. The preparation of such chemically intuitive ansatz may be resource intensive depending on the hardware design and connectivity of the quantum computer. Hardware efficient ansatz are a set of trial wave function which can be quickly prepared on a given quantum computer. One such form of ansatz were used in Ref. [42] to find the ground state energy of several small molecules. These ansatz cut down the requirement of elaborate state preparation. However, they might increase the complexity encountered by the classical optimizer as the ansatz might not systematically approach towards the true ground state. As an extreme example, a hardware efficient wave function prepared by random application of gates is close to a maximally mixed state in the Hilbert space, and classical optimization starting from such state might be hard due to flat energy surface. A systematic approach to generate such hardware efficient ansatz might show promising results on noisy intermediate-scale quantum (NISQ) computers.

#### E. Basis sets

In Appendix A, the starting basis functions  $\{\phi_i\}$  form a complete set. The basis set of the set of all arbitrary wave functions is infinite in size and hence the coefficient matrix  $C$  is infinite dimensional as well. In theory, one can find an exact solution with only  $n$  basis function; this is the basis set where the chosen functions  $\phi_i$  happen to be the solution of HF equations (A5). We also need a finite size basis set to numerically solve the HF equations. A well chosen basis set can still obtain very accurate results with only a finite number of basis functions.

A common starting point for basis functions are the atomic orbital (AO) of hydrogen-like atom. The MOs are linear combination of these AOs. This method is appropriately named linear combination of atomic orbital (LCAO) method. The exact hydrogen-atom like orbital

are represented by Laguerre polynomials. Inspired from these functions, Slater proposed a basis set where the functions decay exponentially in distance,

$$\phi_{\text{STO}}(r; \alpha) \propto p(r)e^{-\alpha r} \quad (\text{E1})$$

where  $p(r)$  is a polynomial in  $r$  and  $\alpha$  is an appropriate scale factor. Such basis functions are called Slater type orbital (STO). While STO accurately describe the shape of the atomic orbitals of an hydrogen-like atom, they are quite cumbersome to use in numerical integration. It is often helpful to use a basis set where the functions decay in exponential of the square of the distances,

$$\phi_{\text{GTO}}(r; \alpha) \propto p(r)e^{-\alpha r^2} . \quad (\text{E2})$$

These basis functions are called Gaussian type orbital (GTO), since they look similar to a Gaussian function. Since multiplication of two GTOs is another GTO, integrals with these functions can be simplified significantly. As a down-side, these functions no longer describe the shape of hydrogen-like orbitals. In order to rectify this problem, basis sets often use a linear combination of GTOs to represent a single AO. A common basis set, STO- $n$ G, employs a combination to  $n$ -GTOs to represent a single STO;

$$\phi_{\text{STO}}(r) \approx \phi_{\text{STO-}n\text{G}} = \sum_{i=1}^n c_i \phi_{\text{GTO}}(r; \alpha_i) \quad (\text{E3})$$

where the parameters  $\{\alpha_i, c_i\}$  are optimized by maximizing the overlap between exact  $\phi_{\text{STO}}$  and the approximate  $\phi_{\text{STO-}n\text{G}}$ .

The STO- $n$ G sets [63] are a minimal basis set, that is, they only use one function to represent an atomic orbital. For example, a carbon atom with five orbitals (1s, 2s, 2p<sub>x</sub>, 2p<sub>y</sub>, 2p<sub>z</sub>) is represented by five functions. This condition, which is well-reasoned based on the physics of the system, usually does not result in good numerical results. We can relax this condition to get better results and use multiple functions to represent the valence orbitals while using a minimal set for the inner electrons. Such basis set is called a split-valence basis set. A double- $\zeta$  set such as the such as cc-pVDZ [64] basis uses two functions for each valence orbital, a triple- $\zeta$  uses three, and so on. The numerical accuracy increases with larger basis sets but more computational resources are required to determine the larger coefficient matrix  $C$  in Eqs. (A2) and (A5).

## F. Qubit tapering

Given a problem Hamiltonian with wave function expressed in a basis of  $M$  spin orbital functions ( $M/2$  spatial orbital functions), the equivalent quantum circuit requires  $M$  qubits, one each to represent an orbital. This number can be reduced by utilizing the symmetry of the problem Hamiltonian and by using approximations that

do not significantly degrade the quality of the variational solution.

The qubit tapering method [65] tries to reduce the number of qubits by systematic identification of internal and spatial symmetry of the second quantized Hamiltonian (2). Since the Hamiltonian preserves the spin and the total number of electrons of the system, one can always remove two qubits from their system via qubit tapering. The method relies on identification of the symmetry generators of the qubit Hamiltonian. After chosen encoding scheme, the qubit Hamiltonian can be written as a sum of Pauli strings,

$$H = \sum_i H_i \prod_{\sigma_i} \sigma_j^\alpha \quad (\text{F1})$$

where  $\alpha \in \{x, y, z\}$  specifies one of the Pauli operators and  $\sigma_j^\alpha \in \sigma_i$  where  $\sigma_i$  is a set of Pauli operators describing the Pauli string of  $i^{\text{th}}$  term. Using techniques adapted from quantum error correction [66, 67], one can find an abelian group  $S$  such that any element of this group commutes with all the Pauli strings of Hamiltonian (F1). The size of generator of the symmetry group  $S$  is the number of qubits that can be tapered from Hamiltonian (F1). In their work, Bravyi et. al. were able to remove two aforementioned qubits as well as another qubit in linear systems such as H<sub>2</sub> and BeH<sub>2</sub>.

We implemented the qubit tapering algorithm for all the dipeptides considered in this work. We started with a stable conformer of each dipeptide obtained from the PubChem database [68] and prepared the respective second quantized Hamiltonian with PySCF [62]. We encoded the second quantized Hamiltonian to its qubit form (Eq. (F1)) with Jordan-Wigner (JW) encoding using the Q# language [69]. Finally, we applied the qubit tapering algorithm. We were not able to eliminate any qubits beyond the aforementioned two qubits from any of the dipeptide. This result is not surprising since dipeptides are disordered systems and do not arrange themselves in a symmetric geometry. Nevertheless, such qubit tapering algorithms might be improved by working on the symmetries of a sub-system of the Hamiltonian (such as a symmetric aromatic ring which is part of a bigger protein chain). We leave this question open for future work.

## G. Common gates

A quantum algorithm starts with a simple many qubit state, usually the  $|0000\dots 0\rangle$  state, and applies various quantum gates which manipulate the qubits accordingly. All quantum gates can be represented by a unitary operator. We can also interpret these gates as rotation on the Bloch sphere. Common single qubits gates are the Pauli gates which rotate the qubits by an angle of  $\pi$  along the

respective axis:

$$\sigma^x = \begin{pmatrix} 0 & 1 \\ 1 & 0 \end{pmatrix}, \quad \sigma^y = \begin{pmatrix} 0 & -i \\ i & 0 \end{pmatrix}, \quad \sigma^z = \begin{pmatrix} 1 & 0 \\ 0 & -1 \end{pmatrix}. \quad (\text{G1})$$

Other common gates are the Hadamard gate  $H$ , the  $Y$  gate and the  $T$  gate,

$$H = \frac{1}{\sqrt{2}} \begin{pmatrix} 1 & 1 \\ 1 & -1 \end{pmatrix}, \quad Y = \frac{1}{\sqrt{2}} \begin{pmatrix} 1 & i \\ i & 1 \end{pmatrix}, \quad T = \begin{pmatrix} 1 & 0 \\ 0 & e^{i\pi/4} \end{pmatrix}. \quad (\text{G2})$$

Two qubit gates can be used to generate entangled pair of qubits. The Controlled-NOT (CNOT) gate is a two qubit gate which applies the  $\sigma^x$  gate to the second (target) qubit only if the first (control) qubit is in state  $|1\rangle$ ,

$$\text{CNOT} = |0\rangle\langle 0| \otimes I + |1\rangle\langle 1| \otimes \sigma^x \quad (\text{G3})$$

where  $I = \text{diag}(1, 1)$  is the single qubit identity matrix. The CNOT gate along with the above mentioned single qubit gates form a universal set of quantum gates, that is, any quantum algorithm (or equivalently, a  $n$ -qubit unitary) can be decomposed into a chain of one and two qubit gates (or equivalently, a tensor product of  $2 \times 2$  and  $4 \times 4$  matrices).